




# CRP inhibits the osteoblastic differentiation of OPCs via the up-regulation of primary cilia and repression of the Hedgehog signaling pathway

Jie Xu<sup>1</sup> · Xiangmei Wu<sup>2</sup> · Huifang Zhu<sup>1</sup> · Yinghua Zhu<sup>3</sup> · Kailong Du<sup>1</sup> · Xiaoyan Deng<sup>1</sup> · Changdong Wang<sup>1</sup> 

Received: 3 July 2023 / Accepted: 5 January 2024 / Published online: 12 February 2024  
© The Author(s), under exclusive licence to Springer Science+Business Media, LLC, part of Springer Nature 2024

## Abstract

Inflammation disrupts bone metabolism and leads to bone damage. C-reactive protein (CRP) is a typical inflammation marker. Although CRP measurement has been conducted for many decades, how osteoblastic differentiation influences molecular mechanisms remains largely unknown. The present study attempted to investigate the effects of CRP on primary cultured osteoblast precursor cells (OPCs) while elucidating the underlying molecular mechanisms. OPCs were isolated from suckling Sprague-Dawley rats. Fewer OPCs were observed after recombinant C-reactive protein treatment. In a series of experiments, CRP inhibited OPC proliferation, osteoblastic differentiation, and the OPC gene expression of the hedgehog (Hh) signaling pathway. The inhibitory effect of CRP on OPC proliferation occurred via blockade of the G1-S transition of the cell cycle. In addition, the regulation effect of proto cilium on osteoblastic differentiation was analyzed using the bioinformatics p. This revealed the primary cilia activation of recombinant CRP effect on OPCs through in vitro experiments. A specific Sonic Hedgehog signaling agonist (SAG) rescued osteoblastic differentiation inhibited by recombinant CRP. Moreover, chloral hydrate, which removes primary cilia, inhibited the Suppressor of Fused (SUFU) formation and blocked Gli2 degradation. This counteracted osteogenesis inhibition caused by CRP. Therefore, these data depict that CRP can inhibit the proliferation and osteoblastic differentiation of OPCs. The underlying mechanism could be associated with primary cilia activation and Hh pathway repression.

**Keywords** C-reactive protein · Inflammation · Hedgehog · Primary cilia · Osteoblastic differentiation

## Introduction

C-reactive protein (CRP) has five identical subunits, developing a planar ring that endows molecular stability to the protein. It is a phylogenetically backward-looking plasma protein [23], providing Ca<sup>2+</sup>-dependent binding to ligands

and damaged cell membranes [40]. Inflammatory cytokines (for instance, TNF- $\alpha$ ) increase CRP generation during an inflammatory response, indicated by the rising levels, a characteristic employed for clinical targets [4, 30, 32, 49, 58]. Several publications have reported the CRP level association with bone mineral density (BMD) [10, 11, 16, 29, 39, 46], nonvertebral fractures [39, 46], and radiographic vertebral fractures [46]. Furthermore, whether CRP can directly affect osteoblastic differentiation and what molecular mechanisms could occur remain unclear.

Primary cilia are non-motor microtubular organelles located on the majority of vertebrate cells (such as osteoblasts and osteocytes) [62] and extend as a solitary unit from the basal body [47]. During cell cycling and proliferation, emerging evidence indicates that the primary cilia act as a unique dynamic organelle carrying signals critical to proliferation [7, 13, 19, 31, 38, 41, 45, 55]. This process is mediated by the ciliary-dependent actions of Gli transcription factors controlling the cell cycle regulator expression [8, 15,

✉ Changdong Wang  
wangchangdong@cqmu.edu.cn

<sup>1</sup> Department of Biochemistry and Molecular Biology, Molecular Medicine and Cancer Research Center, College of Basic Medicine, Chongqing Medical University, Chongqing 400016, China

<sup>2</sup> Department of Physiology, Molecular Medicine and Cancer Research Center, College of Basic Medicine, Chongqing Medical University, Chongqing 400016, China

<sup>3</sup> Department of Pre-Hospital Emergency, Chongqing Emergency Medical Center, Central Hospital of Chongqing University, Chongqing 400014, China

22]. As the cell cycle begins, primary cilia are broken down and assembled in non-dividing cells during the G0/G1 phase [42]. In particular, many studies have observed that primary cilia also regulate skeletal development in adult embryos [3, 5, 17, 18, 36, 48], mechanically controlling bone formation [26, 59]. The ciliary-associated proteins polycystin-1 (Pkd1) and Kif3a impair osteoblastic differentiation [44, 60]. Additional research demonstrated that conditional knockout of Pkd1 or Kif3a impairs the sensory function of osteoblasts while destroying mechanosensory-mediated skeletal homeostasis [52, 59]. However, the mechanism of primary cilia regulating osteoblast proliferation and differentiation during skeletal development is unknown.

Hh signaling is the principal pathway involved in regulating cell function significant for skeletal development and repair [28, 37]. Hh ligands comprise three members: Indian Hh (IHH), Sonic Hh (SHH), and Desert Hh (DHH) [24, 37, 54]. Without the SHH expression, the transporter-like receptor Patched-1 (PTCH1) is concentrated within the ciliary membrane to prevent smoothed (SMO) accumulation. Elevated cAMP enhances the hydrolysis of the full-length form of the Gli transcription factor (Gli-FL) into its repressor form (Gli-R). Conversely, SHH, binding to PTCH1, results in concomitant enrichment and activation of SMO in the cilia [9, 34, 56, 64]. Active SMO leads to the dissociation of the Suppressor of Fused (SUFU) from Gli transcription factors. This allows activated Gli proteins (Gli-A) to create and transduce Hh signals to primary cilia [9, 34, 56, 64], causing transcriptional activation of Hh genes [1]. Primary cilia directly affect the Hh signaling pathway transduction and bone formation. Eduardo et al. observed that IFT88 silencing reduced osteoblastic genes and Hh transcription factor Gli1 within osteocytes and osteoblasts [35]. Suzuki et al. discovered that changes in the number and length of primary cilia in *Dchr7* and *Insig1/2* mutant osteoblasts affected the Hh signal transduction activity, leading to abnormal osteoblastic differentiation [51].

Although CRP levels and other chronic inflammatory mediators have been monitored for decades, little is known about whether CRP can directly affect osteoblast proliferation or differentiation. The current study explored the inhibitory effect of CRP over the proliferation and osteoblastic differentiation of osteoblast precursor cells (OPCs) and the underlying mechanisms.

## Materials and methods

### Cells and cell culture

Primary OPC isolation was performed with procedures approved by the Institutional Animal Care and Use Committee (IACUC) of Chongqing Medical University. 3–4

days old suckling Sprague Dawley (SD) rats were sacrificed by cervical dislocation. The skull was removed on a sterile table, and the periosteum with surrounding connective tissue was discarded. The calvarial bone was rinsed with PBS 4–5 times and then cut into small pieces. The pieces were digested in type I collagenase (EMD, Darmstadt, Germany) and trypsin (Corning, Manassas, VA) at a ratio of 1:1 at 37 °C for 1–2 h. They were centrifuged at 1000 r/min for 5 min using a low-speed medical centrifuge (15011249, Beijing), which retained the pellet. The digested cells were washed, re-centrifuged, and then plated in  $\alpha$ -MEM supplemented with 10% fetal bovine serum (FBS) (Gibco), 100 U/mL penicillin, and 1 mg/mL streptomycin. Osteoblastic differentiation was induced using OS medium consisting of  $10^{-8}$  M dexamethasone (SLBS5298, Sigma, USA), 50  $\mu$ g/mL ascorbic acid (SLBQ0061V, Sigma, USA), and 10 mM  $\beta$ -glycerophosphate (154804-51-0, Sigma, USA).

### Cell treatment

The study used 5 mg/mL recombinant CRP (BBI, D620482-0100, Shanghai) to treat primary OPCs and observe the effect of CRP on osteoblasts. The role of primary cilia was investigated in osteoblastic differentiation after recombinant CRP treatment. Cells were incubated overnight with 10 mM chloral hydrate (BBI, Songjiang, Shanghai, China) to remove the primary cilia. The role of the Hh signaling pathway in osteoblastic differentiation after recombinant CRP treatment was explored by processing primary OPCs using a 10 nM Sonic Hedgehog signaling agonist (SAG, sc-212905, Santa Cruz).

### Cell counting kit 8 (CCK8) assay

CCK8 assay helped evaluate the CRP effect on cell proliferation. OPCs were cultured in 96-well plates ( $2 \times 10^3$  cells/well), and 5 mg/mL of recombinant CRP was added. After 24, 48, and 72 h, 10  $\mu$ L CCK8 solution (Beyotime, China) was added and incubated for 2 h. Finally, cell viability was determined by recording the absorbance at 450 nm with a microplate reader (Thermo, USA).

### Flow cytometry

OPCs were seeded in 6-well plates at  $2 \times 10^5$  cells/well density and then treated with recombinant CRP for 72 h. The supernatant was discarded after centrifugation. OPCs were washed thrice in PBS, and the supernatant was discarded after every wash. After harvesting the OPCs, the cells were fixed overnight in ice-cold 70% ethanol and stained using propidium iodide (Sigma) for 30 min. After staining, a BD FACSAria II (USA) flow cytometer helped assess the cell cycle phase distribution.

The cells were collected, including those floating within the culture medium. Then, 200  $\mu$ L binding buffer was added before the cells were mixed and resuspended. Later, a 5  $\mu$ L aliquot of Annexin V-FITC was added and incubated for 10 min in the dark at room temperature. The cells were centrifuged at 1000 rpm for 5 min, following which the supernatant was discarded. A 200  $\mu$ L aliquot of binding buffer was added to the cells and resuspended before staining using 5  $\mu$ L of propidium iodide (Sigma). The stained CRP-treated cells were analyzed using flow cytometry to determine the apoptosis extent.

### Alizarin red staining

Osteoblastic differentiation was induced with OS medium for 21 days, after which Alizarin Red S solution helped measure the formation of bone nodules. The protocol was followed: adherent OPCs were washed three times using PBS, then fixed with 5% paraformaldehyde for 10 min. Then, they were rinsed with PBS three times, stained with Alizarin Red S, and rinsed twice using deionized water (pH 4.2). After drying at room temperature, the OPCs were imaged with a light microscope. Then, the OPCs were decolorized with 10% (w/v) cetylpyridinium chloride (Sigma) in 10 mM sodium phosphate (pH 7.0) for 10 min. The absorbance at 562 nm of specified aliquots transferred to a fresh 96-well plate was recorded, and the experiment was repeated thrice.

### ALP activity analysis

OPCs were permeabilized with 0.5% Triton X-100. ALP was determined in an alkaline solution (1.5 M, pH 10.3) supplemented with 10 mM p-nitrophenyl phosphate. NaOH solution (0.1 N) helped stop the reaction, after which a microplate reader helped record the optical density at 405 nm. DNA content was used to normalize ALP activity, expressed as nmol of p-nitrophenol produced per mg of total DNA per min.

### Immunofluorescence

12 mm circular micro coverslips (89015-724, VWR, USA) on which cells were cultured were sterilized, dried with ethanol, and then placed inside the wells of a 24-well plate. OPCs were seeded at a density of  $4 \times 10^4$  cells/well and cultured with recombinant CRP (5 mg/mL) for three days. The OPCs were washed with PBS three times, fixed with 4% methanol for 10 min, and then permeabilized with 0.05% Triton X-100. The cells were incubated using 5% BSA for 60 min with a specified antibody panel overnight at 4 °C to avoid non-specific binding. After staining the nuclei with DAPI (1:1000, Sigma), the cells were observed and imaged

using a Leica DM4000 microscope. The experiment was performed in quadruplicate.

Immunofluorescence helped visualize the structure of the primary cilia using antibodies against acetylated  $\alpha$ -tubulin (1:1000, T6793, Sigma),  $\gamma$ -tubulin (1:1000, T3320, Sigma), Gli2 (1:1000, YN3016, ImmunoWay), SUFU (1:1000, C54G2, CST), Ki67 (1:200, Santa Cruz), and Osteocalcin (OCN, 1:1000, 16157-1-AP, Proteintech, USA). Alexa Fluor568-conjugated (1:1000, A-11011, Invitrogen) or Alexa Fluor647-conjugated anti-mouse (1:1000, A-21235, Invitrogen) antibodies were procured as secondary antibodies.

### Western blot analysis

Total protein was extracted from recombinant CRP-treated cells, and its concentration was measured with a bicinchoninic acid (BCA) assay kit (Pierce, Rockford, IL, USA). The proteins were separated using 10% sodium dodecyl sulfate–polyacrylamide gel electrophoresis (SDS-PAGE). Then, they were transferred to polyvinylidene fluoride (PVDF) membranes in a buffer of 192 mM glycine, 25 mM Tris, and 20% methanol. The membranes were blocked using 5% milk and incubated overnight with various primary antibodies at 4 °C against the following epitopes:  $\gamma$ -tubulin (1:1000, T3320, Sigma) and acetylated  $\alpha$ -tubulin (1:1000, T6793, Sigma) for primary cilia staining, OPN (1:200, 225952-1-AP, Proteintech), ALP (1:1000, A5111, Selleckchem), and Collagen Type I (1:1000, 14695-1-AP, Proteintech) to assess osteoblastic differentiation, Gli2 (1:1000, YN3016, ImmunoWay), SHH (1:1000, A5115, Selleckchem), PTCH1 (1:1000, C53A3, CST), and SUFU (1:1000, C54G2, CST) to determine Hh protein expression, and Cyclin D1 (1:1000, 60186-1-LG, Proteintech), Cyclin D2 (1:1000, 10934-1-AP, Proteintech) and Cyclin E (1:1000, 11554-1-AP, Proteintech) to examine cell cycling. GAPDH (1:1000, YT5052, ImmunoWay) demonstrated the internal control. The membranes were incubated using HRP-conjugated goat anti-rabbit IgG (1:5000, A-11034, Novex, Carlsbad, CA) or goat anti-mouse IgG (1:5000, #7074, CST) secondary antibodies at room temperature for 1 h. The protein bands were visualized with a Bio-Rad ChemiDoc™ Touch Imaging System (USA), and the entire experiment was performed in triplicate.

### Selection and GO enrichment analyses of hub genes

Two microarray datasets from the Gene Expression Omnibus (GEO) database were downloaded: the GSE12266 and GSE37558. A total of 778 differentially expressed genes (DEGs) were identified using the R package DESeq2. The MCODE plugin in the Cytoscape software helped determine the 20<sup>+</sup> genes controlled in the key module. From them, 10 were identified as hub genes with the cytoHubba plugin in Cytoscape software. Gene Ontology (GO) analysis helped

explore the functional role of the genes of interest. The identified Hub genes underwent GO analysis with the David tool (<https://david.ncifcrf.gov/>) for comprehensive functional annotations. A false discovery rate (FDR) < 0.05 in GO analysis was selected as the significant enrichment threshold.

### Statistical analysis

All the data are represented as mean  $\pm$  SEM ( $N \geq 3$ ). A student t-test helped compare the difference between the two groups and a two-way ANOVA for multiple group comparisons.  $P < 0.05$  was considered statistically significant. All the statistical analyses were performed using the GraphPad Prism software [43].

## Results and discussion

### Recombinant CRP inhibits the proliferation of OPCs by blocking the cell cycle in the G1-S transition

OPC proliferation treated with various recombinant CRP concentrations (5, 10, and 20 mg/mL) was determined to explore the role of CRP in osteogenesis [14, 25, 63]. Proliferation decreased significantly at recombinant CRP concentrations of 5, 10, and 20 mg/mL with dose-dependent inhibition (Fig. 1A). Apoptosis increased significantly at recombinant CRP concentrations of 10 and 20 mg/mL, dose-dependently (Supplemental Fig. 1). Staining of Ki67, a proliferation marker, was dramatically lower in the CRP group than in the control (Fig. 1B, C). Cell cycling was investigated using immunofluorescence to explore the underlying mechanisms of CRP-mediated OPC proliferation. Cyclins D1, D2, and E are G1 phase-associated proteins. Immunofluorescence depicted that incubation with recombinant CRP decreased the protein expression levels of Cyclins D1, D2, and E in the nuclear region while inhibiting their nuclear translocation (Fig. 1D–F). Western blot analysis also depicted that CRP decreased the levels of G1 phase-associated proteins (Fig. 1G, H). Finally, flow cytometry indicated that OPC percentages in the G2/M phase decreased significantly. However, those in the G0/G1 phase increased in the recombinant CRP-treated group (Fig. 1I, J).

### Recombinant CRP suppresses osteoblastic differentiation

Since inflammation increases bone resorption and inhibits bone formation [33], osteoblastic differentiation of OPCs treated with recombinant CRP was evaluated by culturing OPCs in OS medium with and without recombinant CRP.

After 14 days, OPCs treated with recombinant CRP showed fewer mineralized nodules (Fig. 2A, B). Quantitative measurements depicted that calcium deposits were smaller than in the control group (Fig. 2C). Western blot analysis indicated that protein marker levels of osteoblastic differentiation were lower in recombinant CRP-treated OPCs than in the control, including ALP and OPN (Fig. 2D, E). Fluorescence staining helped evaluate the expression levels of the osteoblastic differentiation marker OCN. On day 3, the OCN expression was significantly lower than in the control group (Fig. 2F, G). Finally, the early osteoblastic differentiation marker ALP activity was evaluated. The data describe that ALP activity was lower in OPCs treated with recombinant CRP after seven days than in the control group (Fig. 2H).

### Recombinant CRP abnormally activates the expression of primary cilia during the osteoblastic differentiation of OPCs

The R package DESeq2 helped identify 778 differentially expressed genes (DEG) before performing GO and KEGG analysis to determine the vital biological processes associated with osteoblastic differentiation. The results depicted that the DEGs were primarily relevant to three biological processes (BPs): negative apoptotic process regulation, inflammatory response, and signal transduction (Fig. 3A). Then, the MCODE plugin in Cytoscape software was used to identify the 20+ genes regulated in the key module. Among them, 10 were identified as hub genes with the cytoHubba plugin in the Cytoscape software. These could be the differentially expressed genes required for osteoblastic differentiation and proliferation (Fig. 3B). Table 1 depicts the description and function of the 10 Hub genes. Microtubule activity was essential for each of these biological processes and cellular components. Since microtubules are a critical component of primary cilia, primary cilia regulate cell cycle processes. They can prevent abnormal cell growth by restricting the cell cycle in studies of the CRP effect on the primary cilia of OPCs [2, 12]. The present study showed more primary cilia on recombinant CRP-treated OPCs than on control OPCs, indicating that CRP abnormally activated primary cilia formation (Fig. 3C–E). Whether CRP influenced primary cilia disassembly or assembly was also investigated. The primary cilia on OPCs treated with 5 mg/mL recombinant CRP were longer (mean:  $5.065 \pm 1.45 \mu\text{m}$ ) than those of control cells (mean:  $2.195 \pm 1.30 \mu\text{m}$ ) (Fig. 3F, G). Thus, CRP positively affected primary cilia assembly in OPCs. Similarly, Western blot analysis also confirmed that incubation in recombinant CRP was accompanied by higher acetylated- $\alpha$ -tubulin and  $\gamma$ -tubulin expression (Fig. 3H, I).

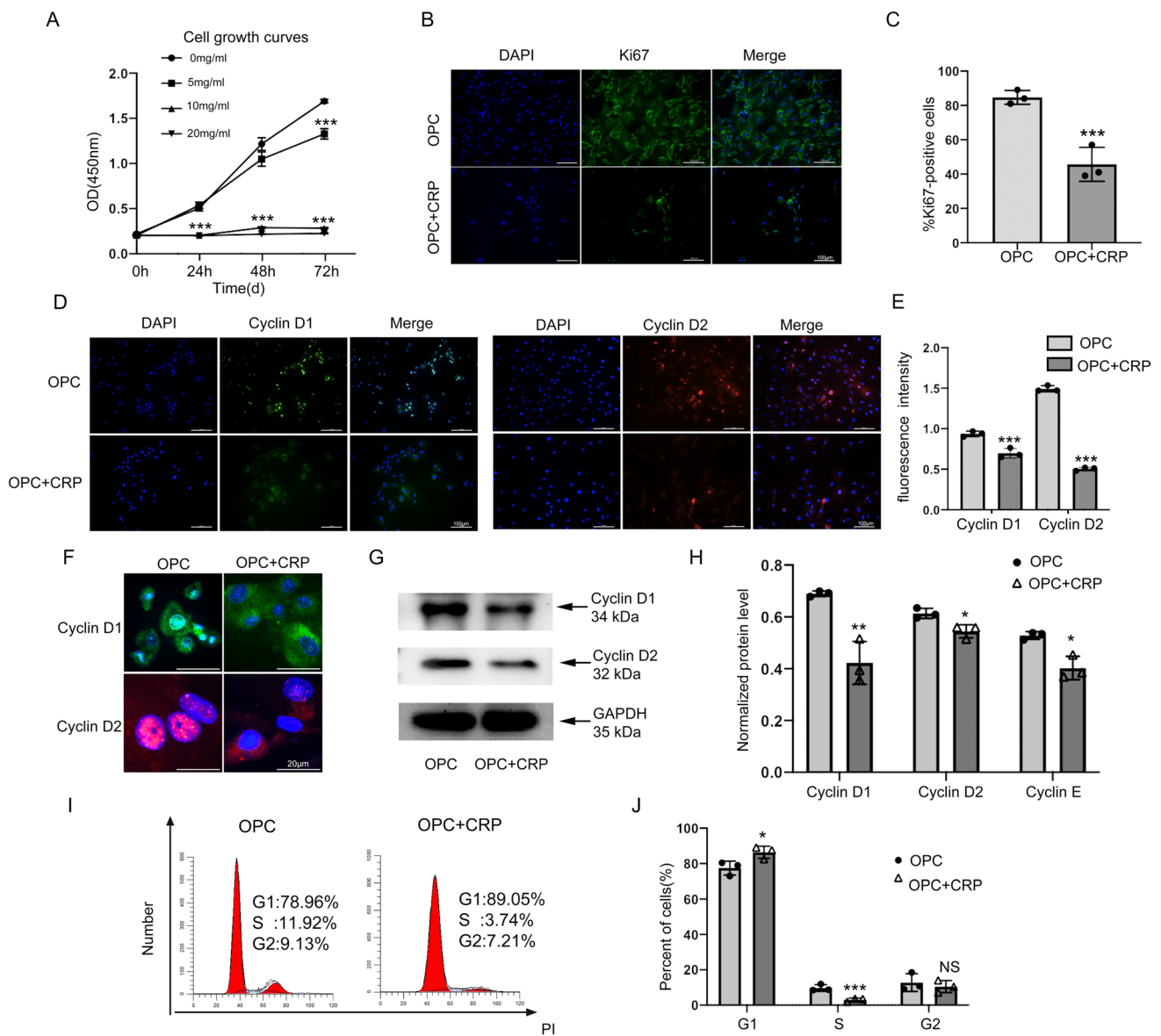


**Fig. 1** CRP inhibits OPC proliferation by blocking the cell cycle at the G1-S transition. OPCs were treated with 5 mg/mL CRP for 3 days ( $n=3$ ). **A** CRP effects on OPC proliferation were evaluated using a CCK8 assay at different CRP concentrations for 24 h, 48 h, and 72 h ( $n=3$ ). **B** Ki67 expression was estimated in OPCs; Nuclei were stained using DAPI. Scale bars: 100  $\mu$ m. **C** Percentage of Ki67-positive cells. The results from five random fields. Scale bars: 100  $\mu$ m. The cell numbers were quantified with Image J. **D** Fluorescence staining of Cyclins D1 and D2 describe their location and expression. Cyclin D1 antibody (green) and D2 antibody (red). Nuclei were stained using DAPI (blue). Scale bars: 100  $\mu$ m. **E** Fluorescence intensity quantification in **(D)**. **F** High-magnification immunofluorescence of Cyclin D1 and D2 in OPCs. Scale bars: 20  $\mu$ m. **G** Western blot analysis depicting Cyclin D1, D2, and E expression in OPCs. **H** Quantitative analysis of Cyclin D1, D2, and E levels from immunoblots in **(G)**. Cyclin D1, Cyclin D2, and Cyclin E levels were normalized to GAPDH. **I** The cell cycle phase distribution after 3D treatment with CRP. **J** CRP-induced OPC cell cycle arrest at G1-S transition. All the data are expressed as mean  $\pm$  SD. The significance is indicated at the following thresholds: \* $p<0.05$ , \*\* $p<0.01$ , \*\*\* $p<0.001$ . The data were analyzed using the student's *t*-test

### Chloral hydrate removes longer primary cilia and rescues the reduction in osteoblastic differentiation of OPCs caused by treatment with recombinant CRP

The cells were treated with chloral hydrate to confirm the changes in primary cilia during the osteoblastic OPC

differentiation, damaging the primary cilia junction with the basal body. Compared with the control group, immunofluorescence staining established that the chloral hydrate successfully removed primary cilia from the OPCs within the recombinant CRP-treated group (Fig. 4A–D). Whether chloral hydrate could enhance osteogenesis was also investigated by assessing the effect

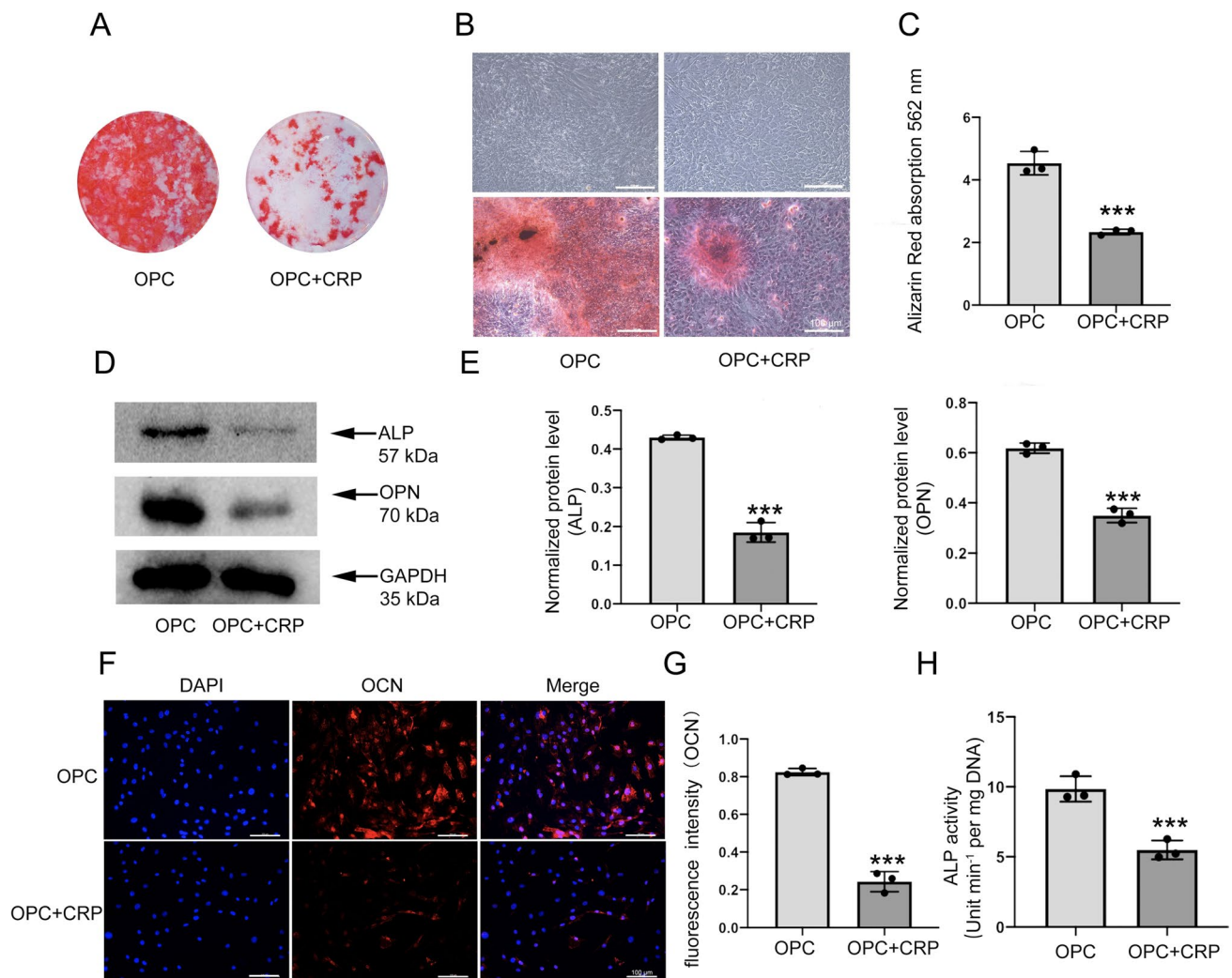


**Fig. 2** CRP suppresses osteoblastic differentiation. **A** Alizarin Red staining of OPCs with or without CRP on day 21 of osteoblastic induction ( $n=3$ ). **B** The representative microscopic images of OPCs stained using Alizarin Red. Scale bars: 100  $\mu\text{m}$ . **C** The mineralization levels depended on Alizarin Red staining ( $n=3$ ). **D** OPCs were treated using 5 mg/mL CRP for 3 days ( $n=3$ ). Western blotting of ALP and OPN in OPCs. **E** Quantitative ALP and OPN protein level analysis using immunoblots in (**D**). ALP and OPN expression levels

were normalized to GAPDH ( $n=3$ ). **F** OPCs were treated using 5 mg/mL CRP for 3 days ( $n=3$ ). Fluorescence staining of OCN location and expression (red). Nuclei stained using DAPI (blue). Scale bars: 100  $\mu\text{m}$ . **G** The fluorescence intensity quantification in (**F**) ( $n=3$ ). **H** ALP activity of OPCs treated with or without CRP on day 7 of osteoblastic induction ( $n=3$ ). The data were analyzed with a student t-test. Error bars: SEM.; \* $p<0.05$ , \*\* $p<0.01$ , \*\*\* $p<0.001$

of chloral hydrate on gene expression involved in OPC osteogenesis. Western blot analysis depicted that, compared with recombinant CRP treatment alone, treatment with recombinant CRP and chloral hydrate (10 mM) for three days led to a marked increase in Collagen Type I and OPN expression levels (Fig. 4E, F). Finally, ALP activity assays described that chloral hydrate significantly rescued the recombinant CRP-mediated reduction in ALP activity (Fig. 4G).

### Recombinant CRP inhibits OPC osteogenesis via the primary cilia/Hh signaling pathway

The Hh pathway plays a significant role in regulating bone formation and osteoblastic differentiation. Recombinant CRP enhanced the protein expression levels of PTCH1 and SUFU in OPCs. However, SAG (10 nM) treatment resulted in promoting SUFU to be partially inhibited, but that of PTCH1 remained unaltered (Fig. 5A). In contrast, recombinant CRP significantly reduced protein expression levels of

Gli2 and SHH in OPCs, while SAG treatment was partially rescued in Gli2. Still, the low SHH expression was unaltered (Fig. 5B). OPCs were treated using chloral hydrate to remove primary cilia and clarify the relationship between primary cilia and the Hh pathway. Later, the difference in Hh pathway activity was observed with or without primary cilia. Chloral hydrate showed the same effect as SAG on the Hh signaling pathway expression (Fig. 5C, D). Gli2, SUFU, and primary cilia were co-stained with immunofluorescence experiments to clarify the relationship. After co-staining acetylated  $\alpha$ -tubulin and Gli2, Gli2 was attached to the bottom of the primary cilia. The expression location was highly coincident with the primary cilia (Supplemental Fig. 2A). The SUFU expression increased with the co-staining of acetylated  $\alpha$ -tubulin and SUFU; however, its site of expression was inconsistent with that of primary cilia (Supplemental Fig. 2B, C). The results indicated that the primary cilia may control the Hh signaling pathway by regulating Gli2 expression. We also investigated whether SAG enhanced osteogenesis. Fluorescence staining depicted that SAG significantly enhanced OCN expression levels, which was decreased due to recombinant CRP treatment (Fig. 5E, F). The SAG influence on gene expression participating in OPC osteogenesis was investigated. Western blot analysis depicted that compared with treatment using recombinant CRP alone, recombinant CRP combined with SAG (10 nM) for three days led to a marked increase in Collagen Type I expression and OPN (Fig. 5G, H). Finally, ALP activity assays depicted that SAG significantly rescued a recombinant CRP-mediated reduction in ALP activity (Fig. 5I). In summary, the results indicated that recombinant CRP inhibited OPC proliferation by preventing G1-S transition of the cell cycle in vitro, inhibited the Hh pathway, and restricted OPCs osteoblastic differentiation by abnormally activating cilia expression.

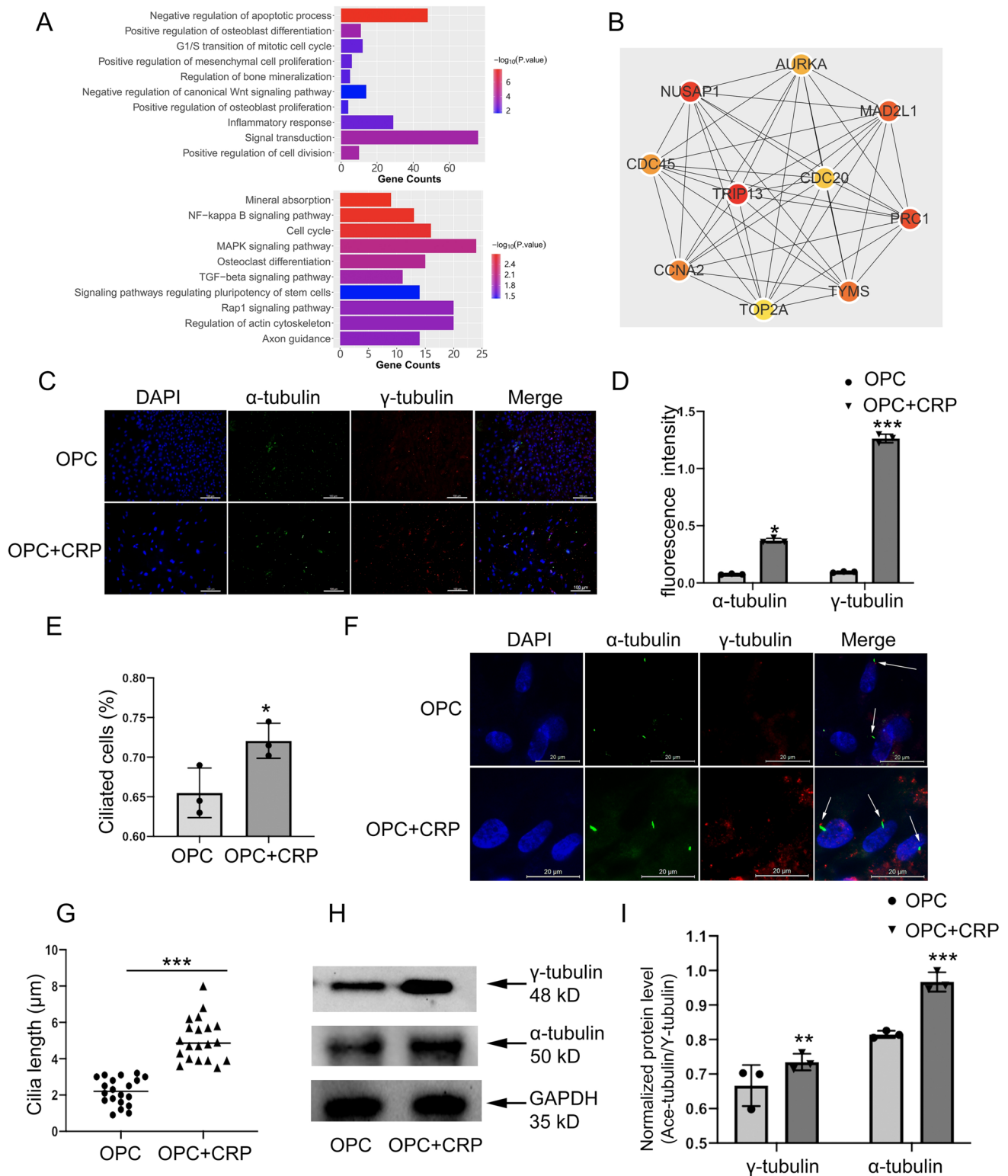
## Discussion

CRP is an inflammatory response factor against infection and tissue damage. The CRP plasma levels are a reliable marker of systemic inflammation. There have been reports published on the association between CRP levels and bone mineral density (BMD) [10, 11, 16, 29, 39, 46], nonvertebral fractures [39, 46], and radiographic vertebral fractures [46]. However, retrospective analyses have not clarified whether CRP directly affects osteoblastic differentiation or is a causal factor. Therefore, the present study treated OPCs using recombinant CRP to observe their effects on osteoblast precursor cells. Thus, recombinant CRP inhibited the cell cycle, proliferation, differentiation, and mineralization of OPCs, reduced the expression of osteoblast-specific genes, and increased the length and number of primary

cilia in OPCs. The addition of SAG (Smoothed agonist) and chloral hydrate (removal of primary cilia) to assess functional gain enabled the salvage of osteoblastic differentiation partially inhibited by recombinant CRP. These findings demonstrate that recombinant CRP could influence the proliferation and cell cycle of OPCs and control the osteoblastic differentiation and mineralization of osteoblasts via the Hh pathway. Primary cilia are critical in this process. For the first time, the current report established that CRP directly regulates osteoblastic differentiation by stimulating primary cilia expression and its influence on the Hh pathway.

There has been little agreement about the effect of CRP on proliferation. CRP has appeared to perform different roles based on the treatments it faces. Wang et al. studied the effect of CRP on the proliferation of vascular smooth muscle cells (VSMs) in a rat carotid artery balloon injury model. They found that CRP enhanced their proliferation in vitro [57]. Yang et al. observed that CRP improved the proliferation of myeloma cells when stressed and protected them from apoptosis caused by drugs [61]. Conversely, Yoshida et al. observed that CRP inhibited the proliferation of activated CD4+ and CD8+ T cells in melanoma patients in vitro. CRP inhibited the expansion of CD8+ T cells in a dose-dependent manner by affecting the T cells [63]. Since the effect of CRP on osteoblast precursor cells has rarely been studied, the present study could be the first to report on its effect on OPCs. This study observed that 5 mg/mL of recombinant CRP inhibited OPC proliferation. Moreover, it significantly enhanced OPC apoptosis with increasing recombinant CRP concentration dose-dependently (Supplemental Fig. 1). Based on the microscopic images of OPCs, 5 mg/mL was the lowest concentration of recombinant CRP exerting a biological effect for subsequent processing. However, recombinant CRP inhibited the expression of Cyclins D1, D2, and E and their nuclear translocation. Additionally, the percentage of cells in the G0/G1 phase significantly increased and decreased in the G2/M phase in recombinant CRP-treated cells, compared with the control group. These findings confirm that recombinant CRP treatment down-regulated levels of G1 phase-associated proteins and induced G1-S transition arrest while inhibiting OPC proliferation.

Recently, Cho et al. observed that CRP decreased the osteoblastic differentiation of MC3T3-E1 cells and inhibited the osteoblast-specific genes *osterix* and *Runx2* expression. No studies have examined CRP's effect on osteoblast precursor cells [6]. While using primary calvarial OPCs is a strength of the present study, a limitation is that these are osteogenic cells from the ectoderm of the neural crest rather than the mesoderm. Interestingly, the findings are like those of Cho et al., who investigated MC3T3.E1 cells derived from calvaria. Consistent with previous studies, the present study demonstrated that CRP inhibited OPC osteogenesis in vitro.



Similarly, recombinant CRP decreased calcium concentrations and protein expression levels of ALP, OPN, and OCN, reducing ALP activity in OPCs undergoing osteoblastic differentiation. When stimulated by the Hh protein, the molecular expression that stimulates osteoblastic differentiation

is regulated by Hh signaling [50, 53]. Similarly, Onodera observed that McCune-Albright syndrome (MAS)-specific human induced pluripotent stem cells (iPSCs) displayed low Hh signal activity and poor mineralization in osteoblast cultures. Osteogenesis was restored to its normal levels by



**Fig. 3** CRP abnormally activates the primary cilia expression during osteoblastic differentiation in OPCs. **A** Bar graph showing the GO and KEGG analysis of differentially expressed genes. **B** Key modules within the network analysis of hub genes. **C** Fluorescent staining depicts the cilia location and expression. OPCs were treated using 5 mg/mL CRP for 3 days ( $n=3$ ). The cilia were stained using  $\gamma$ -tubulin (basal body: red) and acetylated- $\alpha$ -tubulin (axoneme: green) antibodies. Nuclei were stained using DAPI (blue). Scale bars: 100  $\mu$ m. **D** The quantification of fluorescence intensity in (C) ( $n=3$ ). **E** Number of ciliated cells ( $n=3$  with at least 200 analyzed cells) were counted. **F** The representative images of primary cilia in OPCs. Scale bars: 20  $\mu$ m. **G** The calculated length of cilia ( $n=15$  cells) in (F). **H** Acetylated- $\alpha$ -tubulin and  $\gamma$ -tubulin expression in OPCs as observed using Western blotting. **I** Quantitative analysis of protein expression levels from immunoblots in (H). Acetylated- $\alpha$ -tubulin and  $\gamma$ -tubulin expression levels were normalized to GAPDH ( $n=3$ ). The data were analyzed with a student's *t*-test. Error bars: SEM; \* $p<0.05$ , \*\* $p<0.01$ , \*\*\* $p<0.001$

activating small Hh signaling molecules to restore osteoblast precursor cells [6]. The results demonstrated that PTCH1 and SUFU expression were up-regulated, but Gli2 and SHH were down-regulated using recombinant CRP in OPCs. Therefore, recombinant CRP suppresses SHH expression, allowing PTCH1 to prevent SMO accumulation. SUFU

terminally binds to Gli2, preventing Gli2 from undergoing nuclear translocation and causing target gene transcription (Fig. 6②). Thus, adding SAG did not change the expression of PTCH1 or SHH but inhibited SUFU overexpression and increased the low Gli2 expression. SAG mechanisms have been widely investigated. Kanke et al. observed that SAG reduced the expression of osteoblast-related proteins and genes among pluripotent stem cells [27]. Hojo et al. described SAG-induced osteoblastic marker gene expression and osteoblastic differentiation [21]. These reports confirm that recombinant CRP treatment in OPCs inhibits osteoblast differentiation. Thus, adding SAG may induce Hh signaling pathway transduction and partially rescue osteoblastic differentiation (Fig. 6③). Primary cilia could act as a negative regulator of the Hh pathway and as a positive regulator. Ho et al. treated explanted human chondrosarcomas using chloral hydrate and chemically removed the primary cilia from cells. Thus, the primary cilia suppressed Hh signaling in tumor cartilage cells [20]. Consistent with those findings, the study results indicate that treatment with chloral hydrate exhibits an effect like SAG, i.e., Chloral hydrate does not change SHH or PTCH1 expression but inhibits

**Table 1** Descriptions and functions of the 10 Hub genes

Gene.symbol	Description	Function
AURKA	Aurora kinase A	Cell cycle regulating kinases appear to be involved in the formation and/or stability of microtubules at the spindle pole during segregation of chromosomes
NUSAP1	Nucleolar spindle associated protein 1	NUSAP1 is a nucleolar-spindle-associated protein that plays a role in spindle microtubule organization. Proteins related to microtubules that promote the formation of mitotic spindles and microtubules
MAD2L1	Mitotic arrest deficient 2-like protein 1	Component of the spindle-assembly checkpoint that prevents the onset of anaphase until all chromosomes are correctly aligned at the metaphase plate
CDC45	Cell division cycle 45	The protein encoded by this gene was identified by its strong similarity with <i>Saccharomyces cerevisiae</i> Cdc45, an essential protein required for the initiation of DNA replication, important for early steps of DNA replication in eukaryotes
CDC20	Cell division cycle 20	Target of the spindle assembly checkpoint and positive regulator that promotes the complex after mitosis which guides the ubiquitination and degradation of certain proteins in the cell cycle and ensures the normal separation of chromosomes
TYMS	Thymidylate synthase	The encoded thymidylate-forming enzyme (TS) is the rate-limiting enzyme for pyrimidine nucleotide synthesis and an important factor for tumor growth
PRC1	Protein regulator of cytokinesis 1	Proteins involved in cytokinesis are the substrates of several cyclin-dependent kinases (CDK). It is necessary for polarizing parallel microtubules and concentrating factors responsible for contractile ring assembly
CCNA2	Cyclin A2	A protein that binds and activates cyclin-dependent kinase 2 and thus promotes transition through G1/S and G2/M
TRIP13	Thyroid hormone receptor interactor 13	Gene that encodes a protein that interacts with thyroid hormone receptors, also known as hormone-dependent transcription factors. The gene product specifically interacts with the ligand binding domain. This gene is one of several that may play a role in early-stage non-small cell lung cancer
TOP2A	DNA topoisomerase II alpha	This gene encodes a DNA topoisomerase, an enzyme that controls and alters the topologic states of DNA during transcription. This nuclear enzyme is involved in processes such as chromosome condensation, chromatid separation, and the relief of torsional stress that occurs during DNA transcription and replication. It catalyzes the transient separation and rejoining of the two strands of duplex DNA which allows the strands to pass through one another, thus altering the topology of DNA

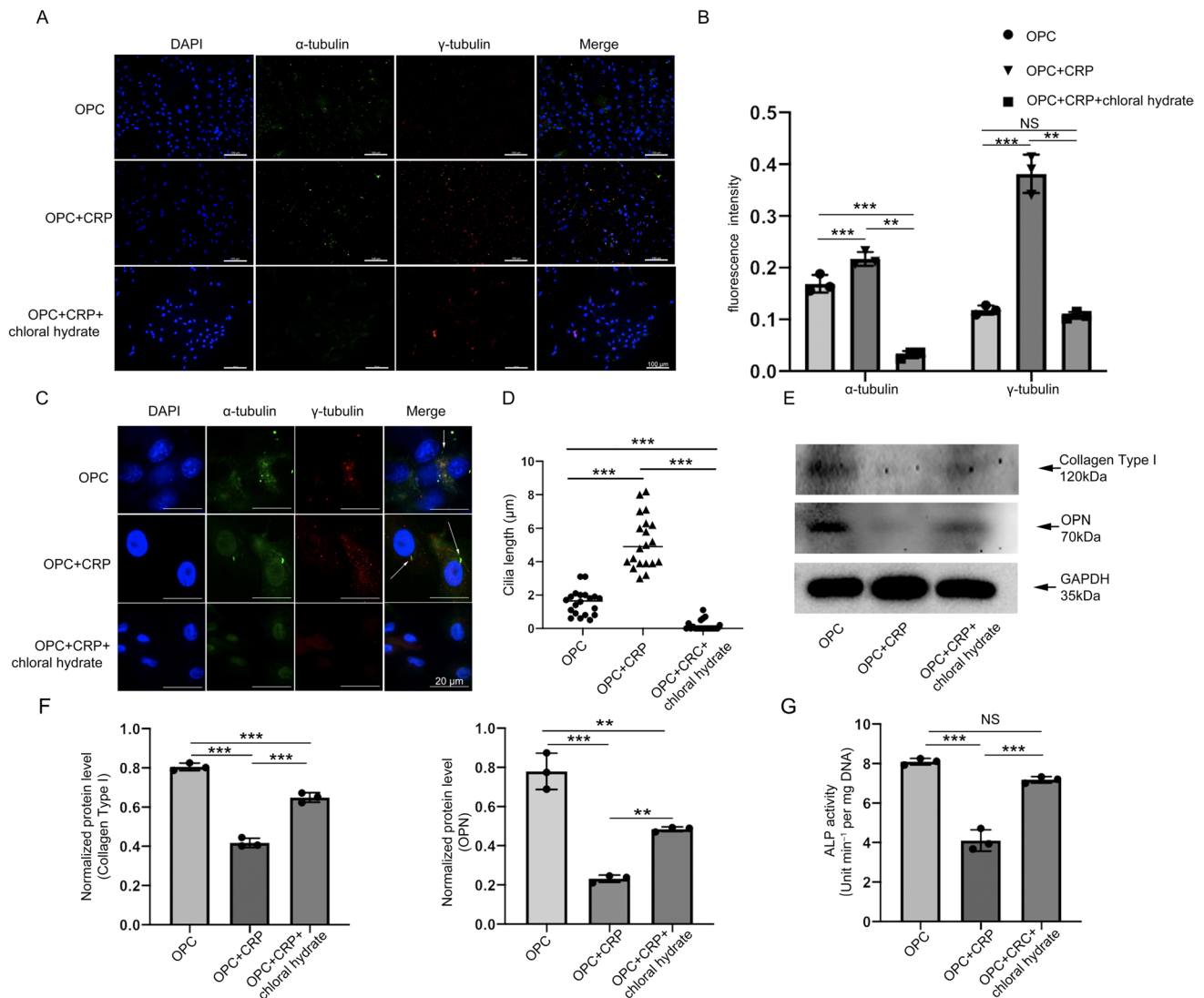


**Fig. 4** Chloral hydrate removes the longer cilia but rescues osteoblastic differentiation reduction of OPCs after CRP treatment. OPCs were cultured in osteoblast medium, CRP, or CRP using chloral hydrate (10 mM) for 3 days. **A** The expression and location of cilia were tested by fluorescent staining. Primary cilia were stained using acetylated- $\alpha$ -tubulin (axoneme, green) and  $\gamma$ -tubulin (basal body, red). Nuclei were stained using DAPI (blue). Scale bars: 100  $\mu$ m. **B** The fluorescence intensity quantification in (A) ( $n=3$ ). **C** The representative images of primary cilia in OPCs. Scale bars: 20  $\mu$ m. **D** The calculated cilia length ( $n=15$  cells) is shown in (C). The expression

levels of osteoblastic differentiation markers were evaluated using Western blotting. **F** The quantitative analysis of collagen-1 and OPN protein expression levels from immunoblots (E). The expression levels of collagen-1 and OPN normalized to GAPDH ( $n=3$ ). **G** The OPCs were cultured in osteoblast medium, CRP, or CRP with chloral hydrate (10 mM) and analyzed for intracellular ALP ( $n=3$ ). All the data are represented as mean  $\pm$  SD. One-way ANOVA using post-mortem testing was performed. The following thresholds represent significance: \* $p < 0.05$ , \*\* $p < 0.01$ , \*\*\* $p < 0.001$ , NS = Not statistically significant

SUFU overexpression and increases the low Gli2 expression. We co-stained Gli2, SUFU, and primary cilia using immunofluorescence experiments to clarify the relationship with primary cilia. Gli2 was attached to the bottom of the primary cilia by co-staining acetylated  $\alpha$ -tubulin and Gli2, the expression site was highly coincident with the primary cilia (Supplemental Fig. 2A). We found that SUFU expression increased by co-staining with acetylated  $\alpha$ -tubulin and SUFU, but its expression site was inconsistent with that of

primary cilia (Supplemental Fig. 2B, C). The results above indicate that the primary cilia may mediate the Hh signaling pathway by regulating Gli2 expression. Thus, treatment with chloral hydrate can eliminate primary cilia and partially restore the Hh signaling pathway, thereby improving osteoblastic differentiation (Fig. 6).

The results indicate that recombinant CRP inhibits OPC proliferation by arresting the G1-S phase of the cell cycle in vitro. Furthermore, recombinant CRP inhibited

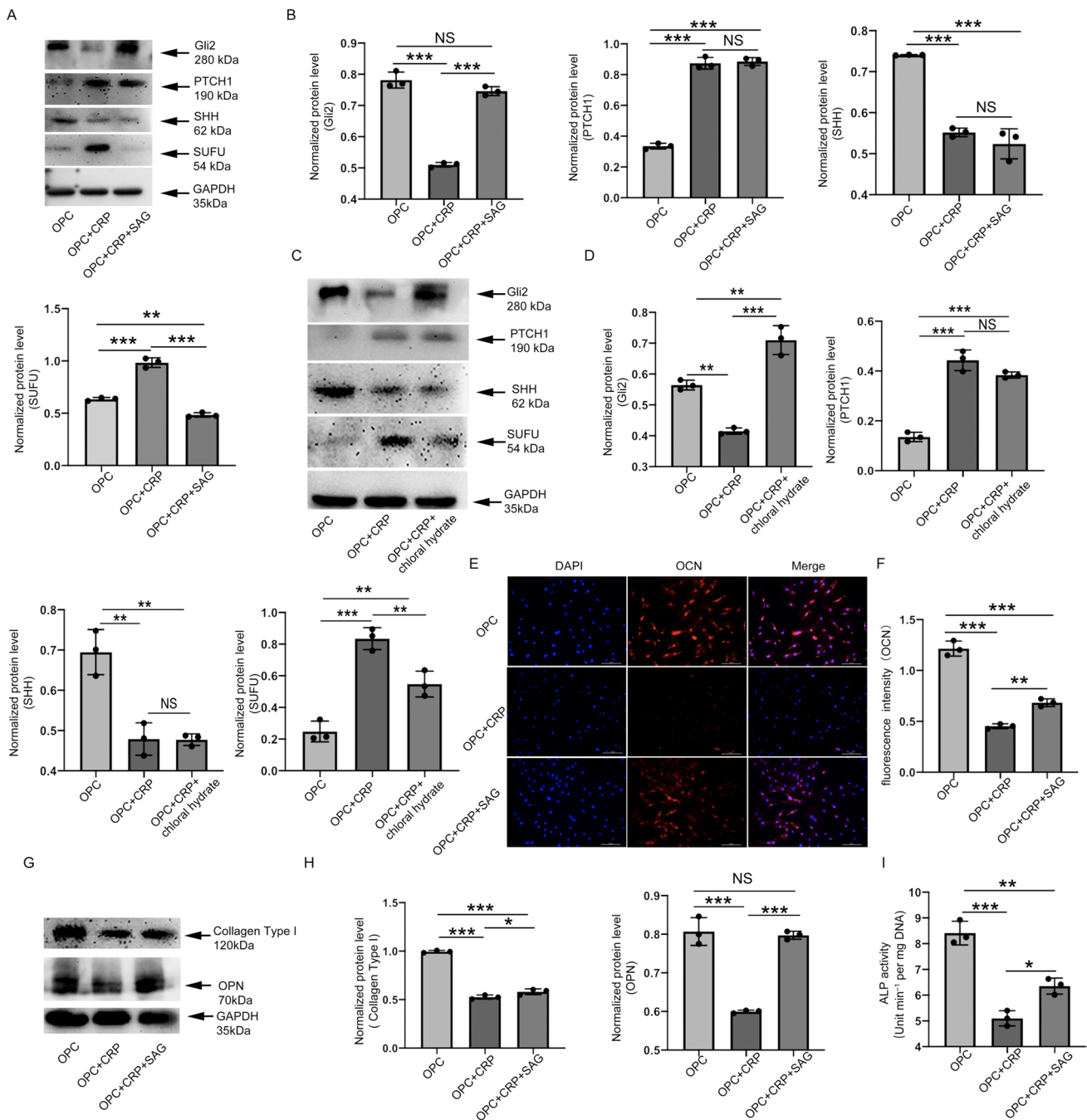


**Fig. 5** CRP inhibits OPC osteogenesis through the cilia/Hh signaling pathway. OPCs were cultured in osteoblast medium, CRP, and CRP with SAG (10 mM) or chloral hydrate (10 mM) for 3 days. **A** The expression levels of Hh pathway proteins were tested using Western blotting. **B** Quantitative analysis of Hh pathway protein levels from immunoblots in (A). Hh pathway protein expression levels were normalized to GAPDH ( $n=3$ ). **C** The expression levels of Hh pathway proteins were tested using Western blotting. **D** Quantitative analysis of Hh pathway protein levels from immunoblots in (C). Hh pathway protein expression levels were normalized to GAPDH ( $n=3$ ). **E** Fluorescence staining of levels and location of OCN expression (red). The

nuclei were stained using DAPI (blue). Scale bars: 100  $\mu$ m. **F** The fluorescence intensity quantification in (E) ( $n=3$ ). **G** The expression levels of osteoblastic differentiation markers tested were using Western blotting. **H** The quantitative analysis of Collagen Type I and OPN levels from immunoblots in (G). Collagen Type I and OPN expression levels were normalized to GAPDH ( $n=3$ ). **I** OPCs were cultured in osteoblast medium, CRP, or CRP with SAG (10nM) for 7 days, and then intracellular ALP activity was measured ( $n=3$ ). All the data are represented as means  $\pm$  SD. One-way ANOVA with post-mortem testing was performed. The significance was recorded with the following thresholds: \* $p < 0.05$ , \*\* $p < 0.01$ , \*\*\* $p < 0.001$

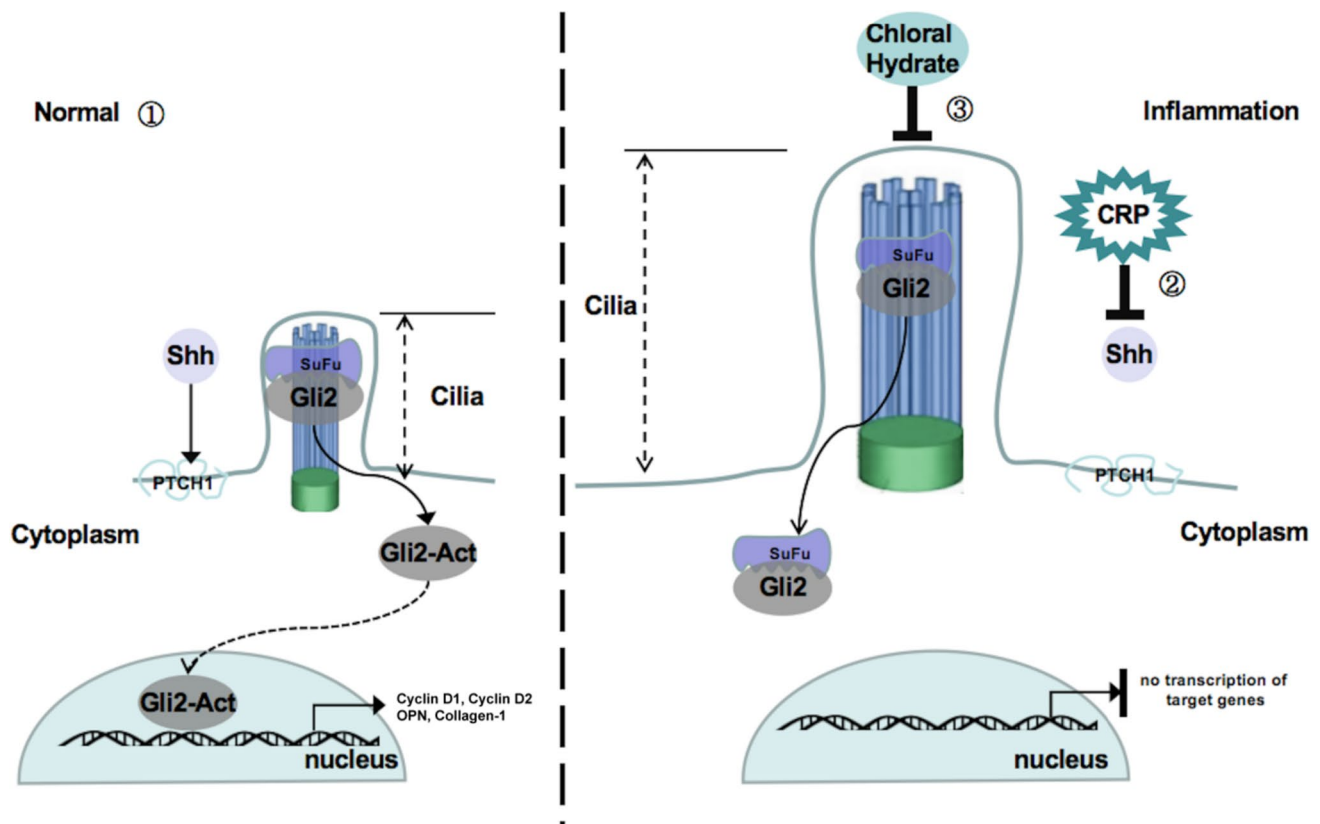


**Fig. 6** Schematic illustration of the Hh pathway function in normal and inflammatory conditions

osteoblastic differentiation of OPCs by inhibiting Hh signaling. We also observed that recombinant CRP-treated primary cilia exhibited higher expression and had a longer length than the control group. Recombinant CRP regulates the Hh pathway by abnormally activating the expression of primary cilia, affecting osteoblast marker genes' expression in OPCs. Adding SAG and chloral hydrate can partially rescue osteoblastic differentiation due to recombinant CRP. The present study's findings represent a novel gene therapy method and drug targets for bone loss diseases caused by inflammation.

**Supplementary Information** The online version contains supplementary material available at <https://doi.org/10.1007/s12032-024-02301-z>.

**Author contributions** CW: Conceptualization, Supervision, Funding acquisition, Methodology. JX: Conceptualization, Investigation, Writing—Original Draft, Funding acquisition. HZ: Supervision. XD: Supervision. XW: Supervision. YZ: Software, Resources. KD: Software.

**Funding** This work was supported by the scientific research project of Chunhui plan in ministry of education the people's republic of china (2022-2 to Changdong Wang); Chongqing Natural Science Foundation of China (Grant CSTB2022NSCQ-MSX0945; cstc2014jcyjA10024 to Changdong Wang); the first scientific research plan of Yuzhong District, Chongqing in 2020 (Grant: 20200112 to Changdong Wang);

the Chongqing Graduate Science and Technology Innovation Project in 2019 (Grant: CYS19204 to Jie Xu); Chinese Higher Education Doctorate Program (Grant: 20125503120015) and Chongqing Education Commission (Grant: CY170402). The content is solely the responsibility of the author and does not necessarily represent the official views of a government with financial support.

**Data availability** Upon request, data to support the results of this study can be obtained from the corresponding author.

## Declarations

**Conflict of interests** The authors declare that there are no conflicts of interest.

## References

1. Alman BA. The role of hedgehog signalling in skeletal health and disease. *Nat Rev Rheumatol*. 2015;11:552–60.
2. Basten SG, Giles RH. Functional aspects of primary cilia in signaling, cell cycle and tumorigenesis. *Cilia*. 2013;2:6.
3. Berbari NF, O'Connor AK, Haycraft CJ, Yoder BK. The primary cilium as a complex signaling center. *Curr Biol*. 2009;19:R526-535.
4. Black S, Kushner I, Samols D. C-reactive protein. *J Biol Chem*. 2004;279:48487–90.

5. Chang CF, Ramaswamy G, Serra R. Depletion of primary cilia in articular chondrocytes results in reduced Gli3 repressor to activator ratio, increased Hedgehog signaling, and symptoms of early osteoarthritis. *Osteoarthr Cartil.* 2012;20:152–61.
6. Cho IJ, Choi KH, Oh CH, Hwang YC, Jeong IK, Ahn KJ, Chung HY. Effects of C-reactive protein on bone cells. *Life Sci.* 2016;145:1–8.
7. Christensen ST, Clement CA, Satir P, Pedersen LB. Primary cilia and coordination of receptor tyrosine kinase (RTK) signalling. *J Pathol.* 2012;226:172–84.
8. Christopher RW. The cilium secretes bioactive ectosomes. *Curr Biol.* 2013;10:906–11.
9. Corbit KC, Aanstad P, Singla V, Norman AR, Stainier DY, Reiter JF. Vertebrate smoothened functions at the primary cilium. *Nature.* 2005;437:1018–21.
10. de Pablo P, Cooper MS, Buckley CD. Association between bone mineral density and C-reactive protein in a large population-based sample. *Arthritis Rheum.* 2012;64:2624–31.
11. Ding C, Parameswaran V, Udayan R, Burgess J, Jones G. Circulating levels of inflammatory markers predict change in bone mineral density and resorption in older adults: a longitudinal study. *J Clin Endocrinol Metab.* 2008;93:1952–8.
12. Eguether T, Hahne M. Mixed signals from the cells antennae: primary cilia in cancer. *EMBO Rep.* 2018. <https://doi.org/10.15252/embr.201846589>.
13. Ezratty EJ, Stokes N, Chai S, Shah AS, Williams SE, Fuchs E. A role for the primary cilium in Notch signaling and epidermal differentiation during skin development. *Cell.* 2011;145:1129–41.
14. Fang Z, Lv J, Wang J, Qin Q, Wang Q. C-reactive protein promotes the activation of fibroblast-like synoviocytes from patients with rheumatoid arthritis. *Front Immunol.* 2020;11:958.
15. Regi G. The zinc-finger transcription factor GLI2 antagonizes contact inhibition and differentiation of human epidermal cells. *Oncogene.* 2004;6:1263–74.
16. Ganesan K, Teklehaimanot S, Tran T, Asuncion M, Norris K. Relationship of C-reactive protein and bone mineral density in community-dwelling elderly females. *J Natl Med Assoc.* 2005;97:329–33.
17. Haycraft CJ, Serra R. Cilia involvement in patterning and maintenance of the skeleton. *Curr Top Dev Biol.* 2008;85:303–32.
18. Haycraft CJ, Zhang Q, Song B, Jackson WS, Detloff PJ, Serra R, Yoder BK. Intraflagellar transport is essential for endochondral bone formation. *Development.* 2007;134:307–16.
19. Heydeck W, Fievet L, Davis E, Katsanis N. The complexity of the cilium: spatiotemporal diversity of an ancient organelle. *Curr Opin Cell Biol.* 2018;55:139–49.
20. Ho L, Ali SA, Al-Jazrawe M, Kandel R, Wunder JS, Alman BA. Primary cilia attenuate hedgehog signalling in neoplastic chondrocytes. *Oncogene.* 2013;32:5388–96.
21. Hojo H, Ohba S, Yano F, Saito T, Ikeda T, Nakajima K, Komiyama Y, Nakagata N, Suzuki K, Takato T, Kawaguchi H, Chung UI. Gli1 protein participates in Hedgehog-mediated specification of osteoblast lineage during endochondral ossification. *J Biol Chem.* 2012;287:17860–9.
22. Hui C-C, Angers S. Gli proteins in development and disease. *Annu Rev Cell Dev Biol.* 2010;27:513–37.
23. Jia Z, Li H, Liang Y, Potempa L, Ji S, Wu Y. Monomeric C-reactive protein binds and neutralizes receptor activator of NF- $\kappa$ B ligand-induced osteoclast differentiation. *Front Immunol.* 2018;9:234.
24. Jiang J, Hui CC. Hedgehog signaling in development and cancer. *Dev Cell.* 2008;15:801–12.
25. Jimenez RV, Wright TT, Jones NR, Jianming W, Gibson AW, Szalai AJ. C-reactive protein impairs dendritic cell development, maturation, and function: implications for peripheral tolerance. *Front Immunol.* 2018;9:372.
26. Kalogeropoulos M, Varanasi SS, Olstad OK, Sanderson P, Gautvik VT, Reppe S, Francis RM, Gautvik KM, Birch MA, Datta HK. Zic1 transcription factor in bone: neural developmental protein regulates mechanotransduction in osteocytes. *FASEB J.* 2010;24:2893–903.
27. Kanke K, Masaki H, Saito T, Komiyama Y, Hojo H, Nakauchi H, Lichtler AC, Takato T, Chung UI, Ohba S. Stepwise differentiation of pluripotent stem cells into osteoblasts using four small molecules under serum-free and feeder-free conditions. *Stem Cell Rep.* 2014;2:751–60.
28. Kimura H, Ng JM, Curran T. Transient inhibition of the Hedgehog pathway in young mice causes permanent defects in bone structure. *Cancer Cell.* 2008;13:249–60.
29. Koh JM, Khang YH, Jung CH, Bae S, Kim DJ, Chung YE, Kim GS. Higher circulating hsCRP levels are associated with lower bone mineral density in healthy pre- and postmenopausal women: evidence for a link between systemic inflammation and osteoporosis. *Osteoporos Int.* 2005;16:1263–71.
30. Kushner I. The phenomenon of the acute phase response. *Ann NY Acad Sci.* 1982;389:39–48.
31. Lancaster MA, Schroth J, Gleeson JG. Subcellular spatial regulation of canonical Wnt signalling at the primary cilium. *Nat Cell Biol.* 2011;13:700–7.
32. Li JJ, Fang CH. C-reactive protein is not only an inflammatory marker but also a direct cause of cardiovascular diseases. *Med Hypotheses.* 2004;62:499–506.
33. Loi F, Córdova LA, Pajarinen J, Lin TH, Yao Z, Goodman SB. Inflammation, fracture and bone repair. *Bone.* 2016;86:119–30.
34. Marigo V, Johnson RL, Vortkamp A, Tabin CJ. Sonic Hedgehog differentially regulates expression of GLI and GLI3 during limb development. *Dev Biol.* 1996;180:273–83.
35. Martín-Guerrero E, Tirado-Cabrera I, Buendía I, Alonso V, Gortázar A, Ardura J. Primary cilia mediate parathyroid hormone receptor type 1 osteogenic actions in osteocytes and osteoblasts via Gli activation. *J Cell Physiol.* 2020;235:7356–69.
36. Martins AA, Paiva A, Morgado JM, Gomes A, Pais ML. Quantification and immunophenotypic characterization of bone marrow and umbilical cord blood mesenchymal stem cells by multicolor flow cytometry. *Transplant Proc.* 2009;41:943–6.
37. McMahon AP, Ingham PW, Tabin CJ. Developmental roles and clinical significance of Hedgehog signaling. *Curr Top Dev Biol.* 2003;53:1–114.
38. Nauli SM, Alenghat FJ, Luo Y, Williams E, Vassilev P, Li X, Elia AE, Lu W, Brown EM, Quinn SJ, Ingber DE, Zhou J. Polycystins 1 and 2 mediate mechanosensation in the primary cilium of kidney cells. *Nat Genet.* 2003;33:129–37.
39. Pasco JA, Kotowicz MA, Henry MJ, Nicholson GC, Spilbury HJ, Box JD, Schneider HG. High-sensitivity C-reactive protein and fracture risk in elderly women. *JAMA.* 2006;296:1353–5.
40. Pepys MB. C-reactive protein: a critical update. *J Clin Investig.* 2003;112:299–299.
41. Phua SC, Lin YC, Inoue T. An intelligent nano-antenna: primary cilium harnesses TRP channels to decode polymodal stimuli. *Cell Calcium.* 2015;58:415–22.
42. Plotnikova OV, Pugacheva EN, Golemis EA. Primary cilia and the cell cycle. *Methods Cell Biol.* 2009;94:137–60.
43. Praetorius HA, Spring KR. Removal of the MDCK cell primary cilium abolishes flow sensing. *J Membr Biol.* 2003;191:69–76.
44. Qiu N, Xiao Z, Cao L, Buechel MM, David V, Roan E, Quarles LD. Disruption of Kif3a in osteoblasts results in defective bone formation and osteopenia. *J Cell Sci.* 2012;125:1945–57.
45. Rohatgi R, Milenkovic L, Scott MP. Patched1 regulates hedgehog signaling at the primary cilium. *Science.* 2007;317:372–6.

46. Rolland T, Boutroy S, Vilayphiou N, Blaizot S, Chapurlat R, Szulc P. Poor trabecular microarchitecture at the distal radius in older men with increased concentration of high-sensitivity C-reactive protein—the STRAMBO study. *Calcif Tissue Int.* 2012;90:496–506.
47. Satir P, Christensen ST. Overview of structure and function of mammalian cilia. *Annu Rev Physiol.* 2007;69:377–400.
48. Serra R. Role of intraflagellar transport and primary cilia in skeletal development. *Anat Rec (Hoboken).* 2008;291:1049–61.
49. Speidl WS, Graf S, Hornykewycz S, Nikfardjam M, Niessner A, Zorn G, Wojta J, Huber K. High-sensitivity C-reactive protein in the prediction of coronary events in patients with premature coronary artery disease. *Am Heart J.* 2002;144:449–55.
50. Spinella-Jaegle S, Rawadi G, Kawai S, Gallea S, Faucheu C, Mollat P, Courtois B, Bergaud B, Ramez V, Blanchet AM, Adelmant G, Baron R, Roman-Roman S. Sonic hedgehog increases the commitment of pluripotent mesenchymal cells into the osteoblastic lineage and abolishes adipocytic differentiation. *J Cell Sci.* 2001;114:2085–94.
51. Suzuki A, Ogata K, Yoshioka H, Shim J, Iwata J. Disruption of *Dhcr7* and *Insig1/2* in cholesterol metabolism causes defects in bone formation and homeostasis through primary cilium formation. *Bone Res.* 2020. <https://doi.org/10.1038/s41413-019-0078-3>.
52. Temiyasathit S, Tang WJ, Leucht P, Anderson CT, Monica SD, Castillo AB, Helms JA, Stearns T, Jacobs CR. Mechanosensing by the primary cilium: deletion of *Kif3A* reduces bone formation due to loading. *PLoS ONE.* 2012;7: e33368.
53. van der Horst G, Farih-Sips H, Löwik CW, Karperien M. Hedgehog stimulates only osteoblastic differentiation of undifferentiated KS483 cells. *Bone.* 2003;33:899–910.
54. Varjosalo M, Taipale J. Hedgehog: functions and mechanisms. *Genes Dev.* 2008;22:2454–72.
55. Veena S. The primary cilium as the cell's antenna: signaling at a sensory organelle. *Science (NY).* 2006;5787:629–33.
56. Wang B, Fallon JF, Beachy PA. Hedgehog-regulated processing of *Gli3* produces an anterior/posterior repressor gradient in the developing vertebrate limb. *Cell.* 2000;100:423–34.
57. Wang CH, Li SH, Weisel RD, Fedak PW, Dumont AS, Szmitko P, Li RK, Mickle DA, Verma S. C-reactive protein upregulates angiotensin type 1 receptors in vascular smooth muscle. *Circulation.* 2003;107:1783–90.
58. Watson J, Round A, Hamilton W. Raised inflammatory markers. *BMJ.* 2012;344: e454.
59. Xiao Z, Dallas M, Qiu N, Nicoletta D, Cao L, Johnson M, Bone-wald L, Quarles LD. Conditional deletion of *Pkd1* in osteocytes disrupts skeletal mechanosensing in mice. *FASEB J.* 2011;25:2418.
60. Xiao Z, Zhang S, Cao L, Qiu N, David V, Quarles LD. Conditional disruption of *Pkd1* in osteoblasts results in osteopenia due to direct impairment of bone formation. *J Biol Chem.* 2010;285:1177–87.
61. Yang J, Wezeman M, Zhang X, Lin P, Wang M, Qian J, Wan B, Kwak LW, Yu L, Yi Q. Human C-reactive protein binds activating Fcγ receptors and protects myeloma tumor cells from apoptosis. *Cancer Cell.* 2007;12:252–65.
62. Yang S, Wang C. The intraflagellar transport protein IFT80 is required for cilia formation and osteogenesis. *Bone.* 2012;51:407–17.
63. Yoshida T, Ichikawa J, Giuroiu I, Laino A, Hao Y, Krogsgaard M, Vassallo M, Woods D, Stephen Hodi F, Weber J. C reactive protein impairs adaptive immunity in immune cells of patients with melanoma. *J immunother cancer.* 2020;8:e000234.
64. Yuan X, Serra RA, Yang S. Function and regulation of primary cilia and intraflagellar transport proteins in the skeleton. *Ann N Y Acad Sci.* 2015;1335:78–99.

**Publisher's Note** Springer Nature remains neutral with regard to jurisdictional claims in published maps and institutional affiliations.

Springer Nature or its licensor (e.g. a society or other partner) holds exclusive rights to this article under a publishing agreement with the author(s) or other rightsholder(s); author self-archiving of the accepted manuscript version of this article is solely governed by the terms of such publishing agreement and applicable law.